

Mathematical analysis of an economic growth model with perfect-substitution technologies*

Paolo Russu

Department of Economics and Business, University of Sassari,
Via Muroni 25, 07100 Sassari, Italy
russu@uniss.it

Received: December 20, 2018 / **Revised:** June 21, 2019 / **Published online:** January 10, 2020

Abstract. The purpose of this paper is to highlight certain features of a dynamic optimisation problem in an economic growth model with environmental negative externalities that gives rise to a two-dimensional dynamical system. In particular, it is demonstrated that the dynamics of the model, which is based on a production function with perfect substitutability (perfect substitution technologies), admits a locally attracting equilibrium with a basin of attraction that may be considerably large, as it can extend up to the boundary of the system phase plane. Moreover, this model exhibits global indeterminacy because either equilibrium of the system can be selected according to agent expectation. Formulas for the calculation of the bifurcation coefficients of the system are derived, and a result on the existence of limit cycles is obtained. A numerical example is given to illustrate the results.

Keywords: dynamic optimisation problem, economic growth model, environmental economics, Hopf bifurcation, Poincaré compactification.

1 Introduction

Equilibrium selection in dynamic optimisation models with externalities may depend on the expectations of economic agents rather than the history of the economy, as pointed out in [22] and [28]. Starting from the same initial values of the state variables (history), economies with identical technologies and preferences may follow rather different equilibrium trajectories according to the economic agents' choices of the initial values of the jumping variables (expectations). As is well known, expectations are important when the dynamical system describing the evolution of the economy admits a locally attracting equilibrium point (which may correspond to a balanced growth path). In that case, if the initial values of the state variables are sufficiently close to the equilibrium values, the transition dynamics depends on the initial choice of the jumping variables, and thus there exists a continuum of equilibrium trajectories that the economy could

*This research was supported by "Fondo di Ateneo per la ricerca 2019".

follow to approach the equilibrium point. This type of indeterminacy, which is known as “local indeterminacy”, has been extensively studied. The analysis of the linearisation of a dynamical system around an equilibrium point provides all the information required to detect local indeterminacy if the equilibrium point is hyperbolic.

However, some studies stress the relevance of global analysis to obtain satisfactory information about the equilibrium selection process. In fact, global analysis allows highlighting more complex contexts in which equilibrium selection is not unequivocally determined by the initial values of the state variables. For example, given the initial values of the state variables, the economy can follow equilibrium trajectories converging to different ω -limit sets, that is, the long-run behaviour of the state variables is rather different along these trajectories [2–4, 6, 12, 14, 20, 29].

The indeterminacy of equilibrium selection is called “global” if it is observed outside the “small neighbourhood” of an equilibrium point to which local analysis techniques are applied.

The present study is based on the model introduced by Antoci et al. [2], who analyse a three-dimensional system (the framework is that introduced in [33]) whose trajectories are suboptimal Nash solutions of a dynamic control problem. Then, in the three-dimensional phase space, the two-dimensional stable manifold of a saddle-point stable stationary state may separate the basin of attraction of another Pareto-dominated stationary state (a poverty trap) from a region whose trajectories tend to a boundary point where the economy collapses (i.e. physical capital and labour tend to zero, whereas the environmental resource tends to its carrying capacity). The possible existence of limit cycles, generated by Hopf bifurcations, is demonstrated through numerical simulations.

In [2], the authors assumed that the production technology is represented by the Cobb–Douglas function $Y(t) = K(t)^\alpha L(t)^\beta E(t)^\gamma$ with $\alpha + \beta + \gamma < 1$ and $\alpha, \beta, \gamma > 0$, whereas in the present study, a linear production function (perfect substitution technologies) is proposed.

This production function with perfect substitutability allows the investigation of system complexity.

In particular:

- (a) It is possible to determinate both the equilibria and the Hopf bifurcation in closed form; see Sections 4.1 and 4.4, respectively.
- (b) The “optimal” control variables $L(t)$ (labour supply) and $C(t)$ (consumption) are constant over time, giving rise to a two-dimensional dynamical system with a “stronger” form of global indeterminacy. Moreover, it is possible to determine the range of the continuum of initial values L_0^i such that the trajectories form (K_0, E_0, L_0^i) approach a stable equilibrium; see Section 4.3.
- (c) No poverty trap is present.
- (d) The dynamics of the model admits a locally attracting equilibrium point that has an unbounded basin of attraction; see Section 5.

The article is organised as follows. In Section 2, we outline the underlining theory of the model. In Section 3, we describe the dynamics. Section 4 is concerned with the analysis of the model. In Section 5, we apply the Poincaré compactification.

2 Model specification

We analyse an economy constituted by a continuum of identical economic agents, and the size of the agent population is normalised to unity. At each instant of time $t \in [0, \infty)$, a representative agent produces an output $Y(t)$ by the following function with perfect substitutability [12, 14, 16]:

$$Y(t) = \alpha K(t) + \beta L(t) + \gamma E(t), \quad (1)$$

where $K(t)$ is the stock of physical capital accumulated by the agent, $L(t)$ is the agent's labour input, and $E(t)$ is the stock of an open-access renewable natural resource. (In modelling production activity based on open-access natural resources, for example, fishery, forestry and tourism, the stock $E(t)$ of the environmental resource is often an input to the production function [5, 8, 25].) We assume that the agent's instantaneous utility function depends on the leisure $1 - L(t)$ and the consumption $C(t)$ of the output $Y(t)$; more precisely, we consider the following additively nonseparable function (a function of this type is used by [7, 21, 31]):

$$U(C(t), L(t)) = \frac{(C(t)(1 - L(t))^\varepsilon)^{1-\eta} - 1}{1 - \eta},$$

where $C \geq 0$ and $0 \leq L \leq 1$ are an individual's consumption and hours worked, respectively, and the positive parameters ε and η denote the weights on utility towards leisure and the inverse of the intertemporal elasticity of substitution in consumption, respectively. The instantaneous utility function $U(C, L)$ is increasing in consumption and decreasing in labour supply at a decreasing rate, that is, $U_C > 0$, $U_L < 0$, $U_{CC} < 0$ and $U_{LL} < 0$. Moreover, we assume that the utility function is concave in C and $1 - L$, that is, $\eta > \varepsilon/(1 + \varepsilon)$.

The total output $Y(t)$ may be allocated to either aggregate consumption or physical capital accumulation. Consumption contributes directly to the current welfare, whereas investment, which increases the current physical capital stock, ensures greater future consumption and welfare. For the sake of simplicity, it is assumed that there is no physical capital depreciation. Hence, the evolution of $K(t)$ may be expressed by the following differential equation:

$$\dot{K}(t) = Y(K(t), L(t), E(t)) - C(t),$$

where $\dot{K}(t)$ is the time derivative of $K(t)$. To model the dynamics of E , we assume that such a stock is composed of homogeneous units and that it changes over time owing to two different flows with opposite and offsetting effects: First, in the absence of any human economically based intervention, the natural resource evolves according to a biotic law of motion that suggests the well-known logistic equation. (The logistic function has been extensively used as a growth function for renewable resources; see, for example, [11, 18].) Second, the natural capital stock is subject to an economically motivated extraction process, or harvesting activity, because this is required for the production of the final good in the economy.

The economy-wide aggregate production $\bar{Y}(t)$ negatively affects the natural resource stock; however, the value of $\bar{Y}(t)$ is considered exogenously determined by the representative agent.

Combining the two flows that affect the evolution of the natural capital stock, we obtain the following law of motion:

$$\dot{E}(t) = E(t)(\bar{E} - E(t)) - \delta\bar{Y}(t), \tag{2}$$

where the parameter $\bar{E} > 0$ represents the carrying capacity of the natural resource, and the parameter $\delta > 0$ measures the negative impact of $\bar{Y}(t)$ on E . (We note that \bar{E} is the value that E would reach as $t \rightarrow +\infty$ in the absence of negative impact owing to economic activity.) Under the specification (2) of the environmental dynamics, the production process in the economy can be interpreted as an extractive activity. Its impact on the natural resource is given by the rate of harvest, which is proportional to $\bar{Y}(t)$. This assumption is common in models of economic dynamics depending on open-access resources; see among others, [8, 9, 15, 30]. Moreover, it has been introduced in economic growth models where a natural resource-intensive sector is considered; see [5, 26].

We assume that the representative agent chooses the functions $C(t)$ and $L(t)$ to solve the following problem:

$$\max_{C(t), L(t)} \int_0^\infty \frac{(C(t)(1 - L(t))^\epsilon)^{1-\eta} - 1}{1 - \eta} e^{-\theta t} dt \tag{3}$$

subject to

$$\begin{aligned} \dot{K}(t) &= \alpha K(t) + \beta L(t) + \gamma E(t) - C(t), \\ \dot{E}(t) &= E(t)(\bar{E} - E(t)) - \delta\bar{Y}(t) \end{aligned}$$

with $K(0)$ and $E(0)$ given, $K(t), E(t), C(t) \geq 0$ and $0 \leq L(t) \leq 1$ for every $t \in [0, +\infty)$. The multiplication of $U(C(t), L(t))$ in (3) involves the rate of time preference $\theta > 0$. The rate of time preference reflects the fact that individuals evaluate today's utility higher than the same utility gain in some future period or the one of their children.

We assume that the accumulation capital $K(t)$ is reversible, that is, we allow disinvestment $\dot{K}(t) < 0$ at some instants of time. Furthermore, we assume that, in solving problem (3), the representative agent considers $\bar{Y}(t)$ to be exogenously determined because economic agents are a continuum, and hence their individual impact on $\bar{Y}(t)$ is null. However, as agents are identical, ex post $\bar{Y}(t) = Y(t)$ holds. This implies that the trajectories resulting from the model are not socially optimal but Nash equilibria because no agent has an incentive to modify his/her choices if the others do not modify theirs.

3 Dynamics

The current value Hamiltonian function associated with problem (3) is [33]

$$H = \frac{(C(t)(1 - L(t))^\epsilon)^{1-\eta} - 1}{1 - \eta} + \Sigma(t)(\alpha K(t) + \beta L(t) + \gamma E(t) - C(t)).$$

The dynamics of the economy is described by the system

$$\dot{K}(t) = \frac{\partial H}{\partial \Sigma(t)} = \alpha K(t) + \beta L(t) + \gamma E(t) - C(t), \quad (4)$$

$$\dot{\Sigma}(t) = \theta \Sigma(t) - \frac{\partial H}{\partial K(t)} = (\theta - \alpha) \Sigma(t) \quad (5)$$

with the constraint

$$\dot{E}(t) = E(t)(\bar{E} - E(t)) - \delta \bar{Y}(t) \quad (6)$$

and the transversality condition

$$\lim_{t \rightarrow +\infty} e^{-\theta t} \Sigma(t) K(t) = 0. \quad (7)$$

We note that the transversality condition has the following interpretation: the total value of wealth (shadow price \times quantity) does not increase at a rate greater than the rate of return to equilibrium.

Remark 1. We note that the adopted utility function implies $C(t) > 0$ and $0 \leq L(t) < 1$. Indeed, to ensure any value of the parameter $\eta > \epsilon/(1 + \epsilon)$, $C(t) = 0$ and $L(t) = 1$ are dropped.

Thus, we should consider the Lagrangian

$$\mathcal{L} = H + \mu(t)L(t), \quad (8)$$

where $\mu(t)$ is the usual piecewise continuous Lagrange multiplier function in \mathbb{R} .

Therefore, $C(t)$ and $L(t)$ satisfy the following conditions:

$$\mathcal{L}_C = H_C = 0, \quad \mathcal{L}_L = H_L + \mu(t) = 0, \quad (9)$$

where

$$H_C = (C(t)(1 - L(t))^\epsilon)^{-\eta} (1 - L(t))^\epsilon - \Sigma(t), \quad (10)$$

$$H_L = -\epsilon (C(t)(1 - L(t))^\epsilon)^{-\eta} C(t)(1 - L(t))^{\epsilon-1} + \beta \Sigma(t), \quad (11)$$

$$\mu(t) \geq 0, \quad \mu(t)L(t) = 0. \quad (12)$$

We should distinguish between a boundary and an interior arc. We will concentrate on the latter case ($0 < L(t) < 1$, that is, $\mu(t) = 0$) because the former ($L(t) = 0$, that is, $\mu(t) \geq 0$) is analysed in Appendix A.

Combining $H_C = 0$ and $H_L = 0$, we obtain

$$C(t) = \frac{\beta}{\epsilon} (1 - L(t)). \quad (13)$$

By equation (5) we have

$$\frac{\dot{\Sigma}(t)}{\Sigma(t)} = \theta - \alpha, \quad (14)$$

whose solution is

$$\Sigma(t) = \Sigma_0 e^{(\theta - \alpha)t}. \quad (15)$$

Thus, we have the following cases:

- (i) $\theta - \alpha > 0$, and thus $\Sigma(t)$ increases indefinitely;
- (ii) $\theta - \alpha = 0$, and thus $\Sigma(t) = \Sigma_0$;
- (iii) $\theta - \alpha < 0$, and thus $\Sigma(t) \rightarrow 0$;

and the transversality condition (7), which can be written as

$$\lim_{t \rightarrow \infty} \Sigma_0 e^{-\alpha t} K(t) = 0. \tag{16}$$

Substituting (13) in (10), we obtain

$$A(1 - L(t))^\phi - \Sigma(t) = 0, \tag{17}$$

where $A := (\beta/\epsilon)^{-\eta}$ and $\phi := \epsilon(1 - \eta) - \eta$. We note that the condition $\eta > \epsilon/(1 + \epsilon)$ implies that $\phi < 0$. By taking the time derivatives on both sides of equation (17), we obtain

$$A|\phi|(1 - L(t))^{-|\phi|-1} \dot{L}(t) - \dot{\Sigma}(t) = 0. \tag{18}$$

By combining this with equations (14) and (17), the law of motion for the agent's labour L is as follows:

$$\dot{L}(t) = \frac{(\theta - \alpha)}{|\phi|} (1 - L(t)), \tag{19}$$

whose solution (if we let $\omega := (\theta - \alpha)/|\phi|$) is

$$L(t) = 1 + (L_0 - 1)e^{-\omega t}. \tag{20}$$

Then, there are three cases:

1. $\omega > 0$ ($\theta - \alpha > 0$), which implies that $L(t) \rightarrow 1$;
2. $\omega = 0$ ($\theta - \alpha = 0$), which implies that $L(t) = L_0$;
3. $\omega < 0$ ($\theta - \alpha < 0$), which implies $L(t) \rightarrow -\infty$.

Thus, considering the law of motion of $\Sigma(t)$, we conclude that the condition $\theta = \alpha$ is necessary for the existence of an equilibrium point. This implies that the time preference is equal to the market interest rate. (In [10, 13, 27], the authors obtained an equilibrium point if the time preference is equal to the market interest rate even in different contexts.) In this case, the choice of the initial condition $0 < L_0 < 1$ implies $L(t) = L_0$ for all t .

Replacing $L(t)$ with L_0 in (13), we obtain

$$C(t) = C_0 = \frac{\beta}{\epsilon}(1 - L_0). \tag{21}$$

Then the dynamical system to be analysed becomes (henceforth, the time argument will be dropped)

$$\begin{aligned} \dot{K} &= \alpha K + \gamma E - \frac{\beta}{\epsilon}(1 - L_0(1 + \epsilon)), \\ \dot{E} &= E(\bar{E} - \delta\gamma - E) - \delta\alpha K - \delta\beta L_0. \end{aligned} \tag{22}$$

Thus, the transversality condition (16) implies that the system is completely determined over time.

Moreover, after the initial conditions of the economy K_0, E_0, L_0 have been chosen, the consumption $C = C_0$ is determined by equation (21).

To understand the condition $\theta = \alpha$, we rewrite the dynamics of co-state (5) as

$$\theta \Sigma = \dot{\Sigma} - \frac{\partial H}{\partial K},$$

which can be interpreted as follows: The second term on the right is the change in the value (utility) of the agent resulting in an infinitesimal change in its capital stock, whereas the first term (gain or loss) is the change in the capital resulting from any change in its shadow price, that is, the price of its competitive equilibrium. The right-hand side is the net output of an infinitesimal unit of capital, valued at its shadow price, given that the rate of the time preference θ of the agent is equal to the interest rate of the equilibrium of the competitive market capital.

4 Model analysis

In this section, we will analyse the equilibrium points, stability and Hopf bifurcations of the dynamical system (22). Furthermore, the model's global indeterminacy will be discussed.

4.1 Equilibria

The equilibrium points are obtained by determining the intersections between the curves with equations

$$\mathcal{F}(E, K) = \alpha K + \gamma E - \frac{\beta}{\epsilon}(1 - L_0(1 + \epsilon)) = 0, \quad (23)$$

$$\mathcal{G}(E, K) = E(\bar{E} - \delta\gamma - E) - \delta\alpha K - \delta\beta L_0 = 0.$$

We have the following proposition.

Proposition 1. *The dynamical system (22) admits at most two equilibrium points: $A = (E_A^*, K_A^*)$ and $B = (E_B^*, K_B^*)$, where*

$$E_i^* = \frac{\bar{E}}{2} \mp \frac{1}{2} \sqrt{\bar{E}^2 - 4 \frac{\delta\beta}{\epsilon}(1 - L_0)}, \quad (24)$$

$$K_i^* = -\frac{\gamma}{\alpha} E_i + \frac{\beta}{\alpha\epsilon}(1 - L_0(1 + \epsilon)) \quad (25)$$

with $i = A, B$.

Proof. The curve $\mathcal{G} = 0$ is a parabola and $\mathcal{F} = 0$ is a straight line. Consequently, these curves have at most two intersections. It is evident from $\mathcal{F} = 0$ that a necessary condition for the existence of any equilibrium point is $1 - L_0(1 + \epsilon) > 0$, that is, $L_0 < \bar{L}_0 := 1/(1 + \epsilon)$. Solving $\mathcal{F}(E, K) = 0$ for K and substituting in $\mathcal{G}(E, K) = 0$, we have the

following quadratic equation:

$$E^2 - \bar{E}E + \frac{\beta}{\epsilon}\delta(1 - L_0) = 0, \tag{26}$$

whose solutions are (24), which together with K_i^* represent the coordinates of the equilibrium points. \square

To state the next proposition, we define the following threshold values:

$$\bar{E} = \bar{E}_{0T}(L_0) := 2\sqrt{\frac{\beta\delta}{\epsilon}(1 - L_0)}, \tag{27}$$

$$\bar{E} = \bar{E}_1(L_0) := \frac{\beta}{\epsilon\gamma}(1 - L_0(1 + \epsilon)) + \frac{\delta\gamma(1 - L_0)}{1 - L_0(1 + \epsilon)}, \tag{28}$$

$$\tilde{L}_0 = \frac{1}{1 + \epsilon} - \frac{\epsilon\gamma(\gamma\delta + \sqrt{\delta(\delta\gamma^2 + 4\beta(1 + \epsilon))})}{2\beta(1 + \epsilon)^2}. \tag{29}$$

Proposition 2. *The equilibrium points of the dynamical system (22) in the (L_0, \bar{E}) -plane are*

- (i) *A and B if and only if (iff) $0 < L_0 < \tilde{L}_0$ and $\bar{E}_{0T}(L_0) \leq \bar{E} \leq \bar{E}_1(L_0)$ (light grey region in Fig. 1(a));*
- (ii) *A iff $L_0 \in (0, \bar{L}_0)$ and $\bar{E} > \bar{E}_1(L_0)$ (dark grey region in Fig. 1(a)).*

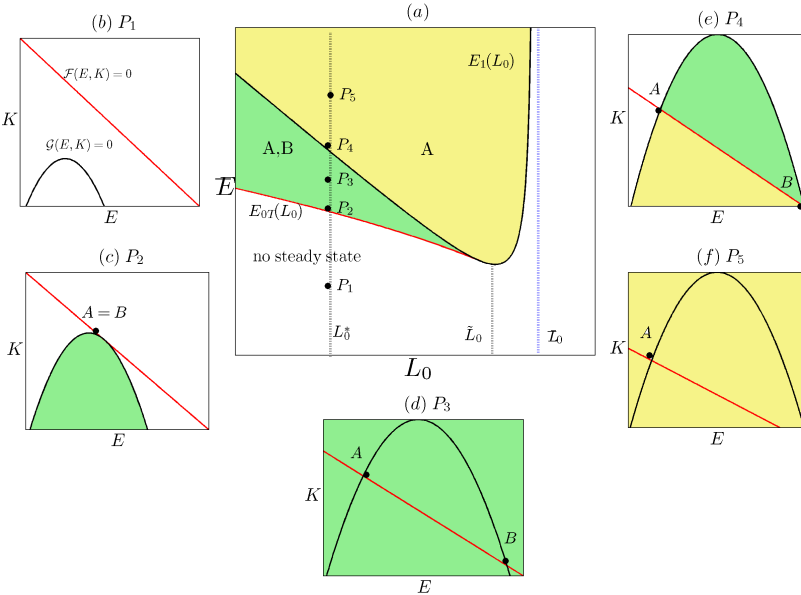


Figure 1. Classification of equilibrium points of (22). Panel (a) shows a numerical simulation of Proposition 2 in the parameter space (L_0, \bar{E}) . Panels (b)–(f) show the graphs of the curves $\mathcal{F} = 0$ (red curve) and $\mathcal{G} = 0$ (black curve), obtained by fixing the parameter L_0 and varying \bar{E} . (Online version in colour.)

Moreover, if $0 < L_0 < \tilde{L}_0$, $\bar{E} < \bar{E}_{0T}(L_0)$, $\tilde{L}_0 < \bar{L}_0$ and $\bar{E} < \bar{E}_1(L_0)$, there are no equilibrium points (white region in Fig. 1(a)).

Proof. The classification in this proposition, based on the values of the parameter \bar{E} and the control L_0 , and represented in the plane (L_0, \bar{E}) (see Fig. 1(a)), can be easily verified considering that the threshold values defined in (27)–(29) are characterised by following properties (which can be easily proved):

- (i) Given L_0 , the function $\bar{E}_{0T}(L_0)$ (see Figs. 1(a) and 1(c)) indicates the value of the parameter \bar{E} such that the curves $\mathcal{F} = 0$ and $\mathcal{G} = 0$ are tangent.
- (ii) Given L_0 , the function $\bar{E}_1(L_0)$ indicates the value of the parameter \bar{E} such that $K_B^* = 0$ (or $\mathcal{G}(E_B^*, 0) = \mathcal{F}(E_B^*, 0)$) (see Fig. 1(e)). This function is convex and presents a vertical asymptote with equation $L_0 = 1/(1 + \epsilon)$; furthermore, it is tangent to the curve $\bar{E}_{0T}(L_0)$ at $L_0 = \tilde{L}_0$; see Fig. 1(a).

Figures 1(b)–1(f) show that given $L_0 = L_0^*$, as \bar{E} increases (from P_1 to P_5 in Fig. 1(a)), the curve $\mathcal{F} = 0$ remains stationary (it does not depend on \bar{E} ; see the first equation in (23)), whereas the curve $\mathcal{G} = 0$ moves upwards, giving rise to: no intersection, a tangent point, two intersections and one intersection between the curves $\mathcal{F} = 0$ and $\mathcal{G} = 0$. \square

4.2 Stability of equilibria

Concerning the stability nature of the equilibrium points, we consider the Jacobian matrix of system (22). More precisely, it is evaluated at any equilibrium point (K^*, E^*) as

$$J = \begin{pmatrix} \alpha & \gamma \\ -\delta\alpha & a \end{pmatrix}, \tag{30}$$

where $a := \bar{E} - \gamma\delta - 2E^*$.

It is well known that the study of the eigenvalues of J is crucial to understand the nature of the equilibrium points. In this respect, the characteristic polynomial of the Jacobian matrix is

$$\mathcal{P}(\lambda) = \lambda^2 - \mathcal{T}\lambda + \mathcal{D},$$

where $\mathcal{T} = \alpha + a$ and $\mathcal{D} = \alpha(\bar{E} - 2E^*)$ represent the trace and the determinant of J , respectively.

It is evident that the signs of both roots of $\mathcal{P}(\lambda)$ depend on the coefficients \mathcal{T} and \mathcal{D} . For instance, under the assumption that $\mathcal{T} > 0$ and $\mathcal{D} > 0$, both roots are positive, and the equilibrium point (K^*, E^*) represents a repellor, whereas if $\mathcal{D} < 0$, then the roots have opposite signs and the equilibrium point is a saddle point.

Under the conditions of the previous proposition, the stability of the equilibrium points A and B can be determined through the signs of \mathcal{T} and \mathcal{D} using the following proposition.

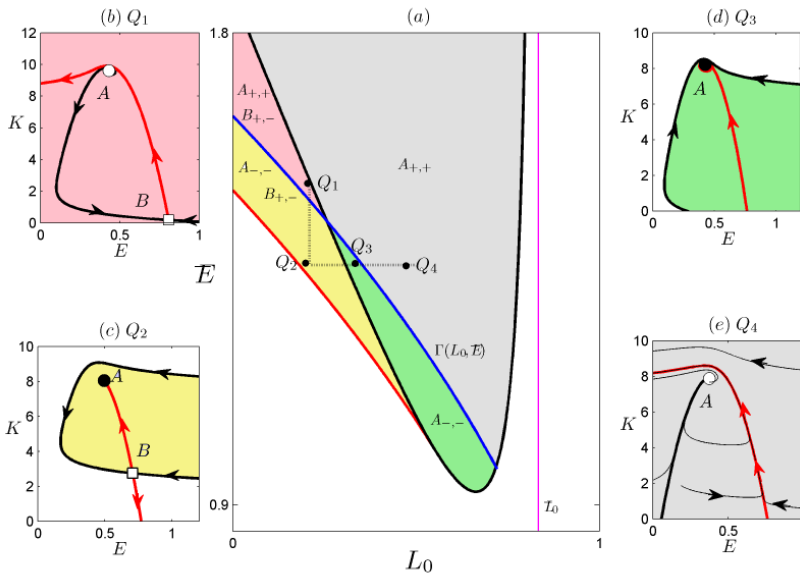


Figure 2. (a) Dynamical behaviour regions for system (22). (b)–(e) Characteristic phase diagrams exemplifying these regions. The pairs of symbols $(-, -)$, $(+, -)$ and $(+, +)$ represent attractive, saddle, and repeller points, respectively. The parameter values are: $\alpha = 0.02$, $\beta = 0.15$, $\delta = 0.75$, $\epsilon = 0.2$ and $\gamma = 0.5$. (Online version in colour.)

Proposition 3. For any coordinates (\bar{E}, L_0) , we consider the curve with equation

$$\Gamma(\bar{E}, L_0) := \alpha - \delta\gamma + \sqrt{\bar{E}^2 - 4\frac{\delta\beta}{\epsilon}(1 - L_0)} = 0, \tag{31}$$

where $0 < L_0 < \bar{L}_0$ (see Fig. 2). Then

- (i) Below this curve, the equilibrium point A is an attractor point;
- (ii) Above this curve, the equilibrium point A is a repeller point.

Moreover, the equilibrium point B is always a saddle point.

Proof. As the equilibrium point A is a point of tangency between the curves \mathcal{F} and \mathcal{G} (see Fig. 2(c)), and $E_T = E/2$, we have $E_A^* < E_T$, whereas for the equilibrium point B , we have $E_B^* > E_T$. Thus, the determinant \mathcal{D} evaluated at A and B is strictly positive and negative, respectively.

Then, the sign of the trace will determine the signs of the real part of the eigenvalues associated with the Jacobian matrix. That is,

Equilibrium point A.

1. $E_A^* < (\bar{E} - \gamma\delta)/2$ implies that $a > 0$. Then $\mathcal{T} > 0$ and $\mathcal{D} > 0$, and hence A is a repeller.
2. $E_A^* > (\bar{E} - \gamma\delta)/2$ implies that $a < 0$. Then $\mathcal{D} > 0$, and hence

- 2.1 if $\alpha + a < 0$, then A is an attractor;
 2.2 if $\alpha + a > 0$, then A is a repellor.

Noting that the trace \mathcal{T} evaluated at E_A^* represents on the (\bar{E}, L_0) -plane the curve with equation (31), we have proved the first part of the proposition.

Equilibrium point B. As $\mathcal{D} < 0$ holds, B is a saddle point.

This completes the proof of the proposition. \square

Figures 2(b)–2(e) show on the (E, K) -plane some numerical simulations of trajectories starting from different initial values of the state variables $K_0 = K(0)$ and $E_0 = E(0)$.

We consider the point Q_1 with coordinates (\bar{E}^1, L_0^1) , lying in the dark yellow region. Then A and B are a repellor and an attractive point, respectively. Numerical examples of trajectories are shown in Fig. 2(b); one of the trajectories (black curve) is the stable manifold of B .

We now consider the point $Q_2 = (\bar{E}^2, L_0^2)$ with $L_0^2 > L_0^1$ and $\bar{E}^2 < \bar{E}^1$ in the region yellow. Then A and B are attractive and repulsive points, respectively. Fig. 2(c) shows numerical examples of trajectories that are the stable and unstable manifolds of the saddle point B .

Furthermore, choosing the point $Q_3 = (\bar{E}^3, L_0^3)$ with $L_0^3 > L_0^2$, only the equilibrium point A can be reached (Fig. 2(d)). The basin of attraction of A is limited by the 1-dimensional stable manifold of the saddle point B .

Finally, a further increase in L_0 ($Q_4 = (\bar{E}^4, L_0^4)$ in Fig. 2(a)) causes (ceteris paribus) the saddle point B to disappear, whereas A becomes a repellor. Accordingly, no equilibrium points can be reached, and all trajectories tend to $K = 0$ and/or $E = 0$ in finite time.

Further analysis of Fig. 2(a) suggests two interesting properties of the model: global indeterminacy and possible existence of limit cycles.

In the next subsection, we will analyse these properties.

4.3 Global indeterminacy

If a value of the parameter \bar{E} is set, then there exists a continuum of values of the parameter L_0 in the yellow region, causing the trajectories to converge to the attractive equilibrium A (indeed, if L_0 lies on the red curve, the trajectory converges to the saddle point B). As A depends on the parameter L_0 , the coordinates of this attractive equilibrium point will vary, and thus the model exhibits global indeterminacy. Therefore, the continuum of values of L_0 (for a suitable value of the parameter \bar{E}) that determines global indeterminacy is included between the curves with equations $\bar{E} - \bar{E}_{0T}(L_0) = 0$ and $\Gamma(\bar{E}, L_0) = 0$ defined in (27) and (31), respectively.

In Fig. 3, all the trajectories lying on the $L_0 = L_{0,i}$ planes start from the same initial values K_0, E_0 belonging to the blue line.

In particular, Fig. 3(a) shows a numerical simulation of global indeterminacy (i.e. there exists a unique value of L_0 such that the red trajectory approaches the saddle point B), whereas Fig. 3(b) shows a numerical simulation of local indeterminacy (i.e. there exists no value of L_0 such that the trajectory approaches B).

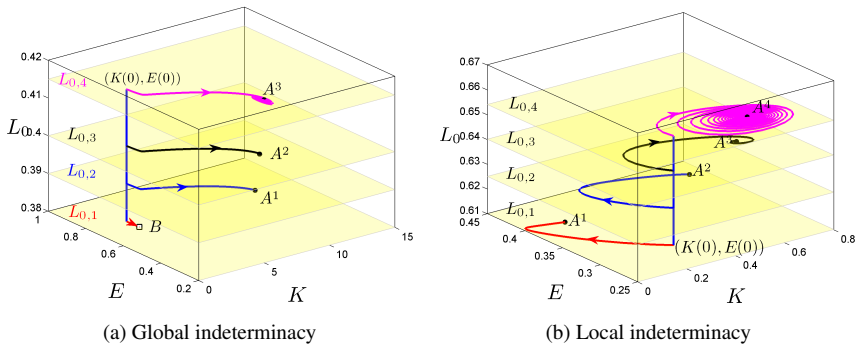


Figure 3. Numerical simulation of global/local indeterminacy. All the trajectories lying on the $L_0 = L_{0,i}$ planes start from the same initial values K_0, E_0 belonging to the blue line. Panel (a) $\epsilon = 0.2, \bar{E} = 1.2$; panel (b) $\epsilon = 0.35, \bar{E} = 9.95$. The other parameters are the same as in Fig. 2. (Online version in colour.)

Remark 2. We note that this global/local indeterminacy is “stronger” than that of the model in [2]. Indeed in [2], if the economy starts from initial values K_0 and E_0 sufficiently close to the stable equilibrium point P_1^* , then there exists a continuum of initial values L_0^1 such that the trajectory from (E_0, K_0, L_0^1) converges to the same values P_1^* (i.e. the coordinates of the attractive equilibrium point do not change).

4.4 Hopf bifurcation

In Fig. 2(a), it is seen that as the attractive point A crosses the curve $\Gamma(L_0, \bar{E})$ (blue curve), its stability nature changes, giving rise to a possibly generic Hopf bifurcation; thus, limit cycles may be obtained.

Regarding this, we state the following proposition.

Proposition 4. *Under our assumptions, a Hopf bifurcation occurs and is supercritical (i.e. an attracting limit cycle is obtained around A when this becomes a repellor).*

Proof. See Appendix B. □

Figure 4 shows numerical simulations of limit cycles around A (which is a repellor) with varying \bar{E} or L_0 .

In Fig. 4(a), for a given value of L_0 , we take \bar{E} as a bifurcation parameter. Then passing from point Q_2 to point Q_1 , we cross the curve Γ , generating a Hopf bifurcation at $\bar{E}_H^1 = 0.1231546$. Figure 4(b) shows limit cycles obtained by increasing the carrying capacity from \bar{E}_H^1 to \bar{E}_H^3 .

Figure 4(d) shows limit cycles obtained by increasing the control L_0 from L_{0H}^1 to L_{0H}^3 , giving rise to a Hopf bifurcation at $L_{0H}^1 = 0.409253$ when we cross the curve Γ as we pass from point Q_3 to point Q_4 .

Moreover, Fig. 4 shows the temporal evolutions of the resource stock $E(t)$ (Figs. 4(a) and 4(d)) and the temporal evolutions of the capital stock $K(t)$ (Figs. 4(c) and 4(f)).

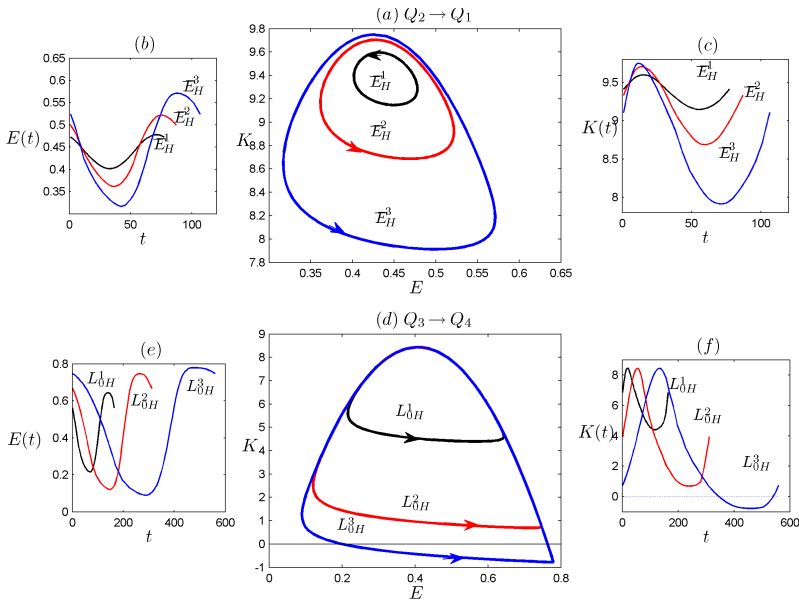


Figure 4. Locally attracting limit cycles “around” A with varying \bar{E} (panel (a)) and L_0 (panel (d)). The cyclical strategy in the time domain is shown around the central figures. The parameter values are the same as in Fig. 1. (Online version in colour.)

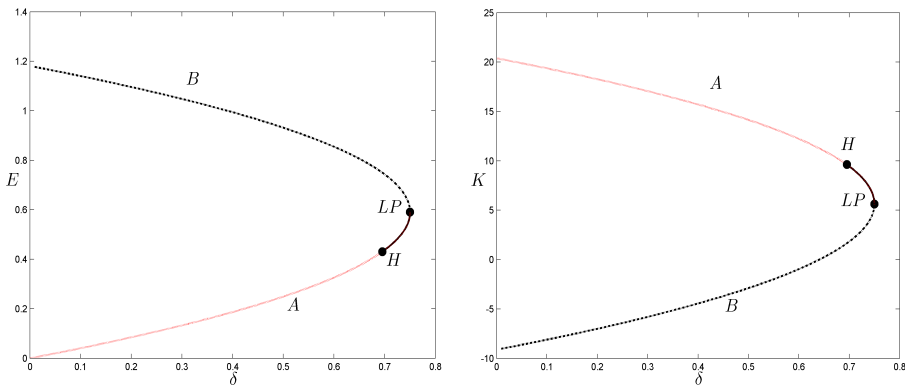


Figure 5. Curve of equilibrium point values of K and E with varying δ . LP denotes limit points and H is a Hopf point. Dotted line: repeller; solid line: attractive point; dashed-dotted line: saddle point. Parameter values: $\alpha = 0.02$, $\beta = 0.15$, $\gamma = 0.5$, $\epsilon = 0.2$, $\bar{E} = 1.18$, $L_0 = 0.32$. (Online version in colour.)

It is interesting to note that the limit cycles L_{0H}^3 cross the line $K = 0$; see Fig. 4(e). This does not happen if we pass from Q_2 to Q_1 because the one-dimensional stable manifold of the equilibrium point B “contains” the limit cycles.

Figure 5 shows the effect of the parameter δ , which measures the environmental impact of the production process, on the equilibrium points K and E . The coordinates

of A are indicated by a solid line (dotted line) if it is an attractive point (repellor), whereas the coordinate of B (which is always a saddle point) are indicated by a dashed-dotted line.

We note that a Hopf bifurcation (indicated by H) occurs when δ is sufficiently large (this is in accordance with [2]).

5 Poincaré compactification

In this section, we analyse the basin of attraction of the equilibrium point A .

Proposition 5. *We assume that there exist two equilibrium points: an attractor A and a saddle point B . Then the basin of attraction of A is unbounded; see Fig. 2(c).*

Proof. We will perform an analysis of the flow of the system (22) at infinity.

Specifically, we will study the Poincaré compactification of the system (22) in the local charts U_i and V_i , $i = 1, 2$. (For the sake of completeness, this is described in detail in Appendix D.)

We write the polynomial differential system (22) as

$$\begin{bmatrix} \dot{x} \\ \dot{y} \end{bmatrix} = \begin{bmatrix} P(x, y) \\ Q(x, y) \end{bmatrix} = J \begin{bmatrix} x \\ y \end{bmatrix} + \begin{bmatrix} 0 \\ G(x, y) \end{bmatrix},$$

where J is the Jacobian matrix (30) and $G(x, y) = -y^2$ is the nonlinear part of (22).

In the local charts U_1 and V_1 . By Appendix D, the expression of the Poincaré compactification $p(X)$ of (22) in the local chart U_1 is

$$\begin{aligned} \dot{u} &= v^2 \left(-u \left(\frac{\alpha}{v} + \gamma \frac{u}{\delta} \right) + a \frac{u}{v} - \delta \frac{\alpha}{v} - \left(\frac{u}{v} \right)^2 \right), \\ \dot{v} &= -v^3 \left(\alpha \frac{1}{v} + \gamma \frac{u}{v} \right), \end{aligned}$$

which can be rewritten as

$$\begin{aligned} \dot{u} &= -\alpha uv - \gamma u^2 v + a uv - \delta \alpha v - u^2, \\ \dot{v} &= -\alpha v^2 - \gamma uv^2. \end{aligned} \tag{32}$$

Then $O_1 = (0, 0)$ is an infinity point. As both the trace and the determinant of the Jacobian matrix of system (32) at the point O_1 are zero, but the Jacobian is non zero, the point O_1 is called nilpotent. The study of its local phase portrait requires Andreev’s nilpotent theorem; see [1].

By rescaling time as $t = -\delta \alpha \tau$, it is easy to see that (32) becomes

$$\begin{aligned} \dot{u} &= v + X(u, v) = v + (pu^2 + qu^2 v + qsvu), \\ \dot{v} &= Y(u, v) = rv^2 + sv^2 u, \end{aligned}$$

where $p = 1/(\delta \alpha)$, $q = a/(\delta \alpha)$, $s = \gamma/(\delta \alpha)$ and $r = \alpha/(\delta \alpha)$.

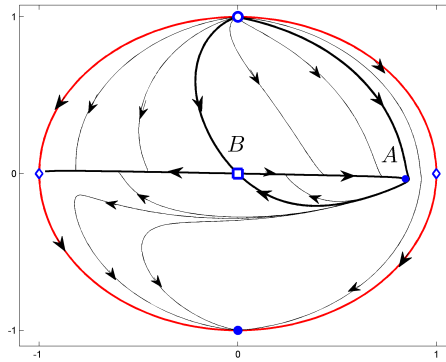


Figure 6. Poincaré disk with stable and unstable separatrices of system (B.1): \diamond : nonelementary point, \square : saddle point, \bullet : stable point, \circ : unstable point. (Online version in colour.)

After straightforward but tedious computations, one obtains

$$\begin{aligned} f(u) &= ra^2u^4 + O(u^5), \\ \phi(u) &= 2au + O(u^2). \end{aligned}$$

Hence, as $\alpha = 4$ is even, $\beta = 1$ and $\alpha > 2\beta + 1$, the nature of the stability of the nilpotent point O_1 is determined by $a.1)$ of the nilpotent theorem; see Appendix E.

The flow in the chart V_1 is the same as that in the local chart U_1 by reversing time because the compactified vector field $p(X)$ in V_1 coincides with the vector field $p(X)$ in U_2 multiplied by -1 .

In the local charts U_2 and V_2 . The differential system on the chart U_2 is

$$\begin{aligned} \dot{u} &= v(\alpha uv + \gamma v - auv + \delta\alpha u^2v + u), \\ \dot{v} &= -v(av - \delta\alpha uv - 1), \end{aligned} \tag{33}$$

where $O_2 = (0, 0)$ is an infinity point. As both the trace and the determinant of the Jacobian of the system (33) are strictly positive, O_2 is a repeller.

The flow in the chart V_2 is the same as that in the local chart U_2 by reversing time because the compactified vector field $p(X)$ in V_2 coincides with the vector field $p(X)$ in U_2 multiplied by -1 . Hence, the infinity point in the chart V_2 is an attractor. \square

Figure 6 shows a numerical simulation of the above proposition, highlighting the stable and unstable separatrices as well as the unbounded basin of attraction of the equilibrium point A . The parameters of this simulation are as in Fig. 2(c).

Acknowledgment. The author would like to express their sincere appreciation to the anonymous reviewers for their significant suggestions from which the paper has been substantially improved.

Appendix A: Boundary arc $L(t) = 0$

If $L(t) = 0$, the necessary conditions (9)–(11) become

$$C(t)^{-\eta} - \Sigma(t) = 0, \tag{A.1}$$

$$-\epsilon C(t)^{-\eta+1} + \beta \Sigma(t) + \mu(t) = 0 \tag{A.2}$$

in addition to the complementary slackness condition (12) and the solution of the differential equation of the co-state dynamics (5)

$$\Sigma(t) = \Sigma_0 e^{-mt}, \tag{A.3}$$

where $m := \alpha - \theta$ and Σ_0 is the initial condition.

To derive an explicit formula for the Lagrange multiplier $\mu(t)$ along the boundary arc, we can use (A.2) combined with (A.1), yielding

$$\mu(t) = (\epsilon C(t) - \beta) \Sigma(t).$$

By the nonnegativity condition in (12) we have

$$C(t) \geq \frac{\beta}{\epsilon}.$$

By equations (A.1) and (A.3), the time evolution of consumption C is

$$C(t) = C_0 e^{mt/\eta} \tag{A.4}$$

with the initial condition $C_0 = (1/\Sigma_0)^{1/\eta}$. Combining this with the transversality condition (7) and the corresponding state equations

$$\dot{K}(t) = \alpha K(t) + \gamma E(t) - C(t), \tag{A.5}$$

$$\dot{E}(t) = E(t)(\bar{E} - \delta\gamma - E(t)) - \delta\alpha K(t), \tag{A.6}$$

we obtain the dynamical system to be analysed.

It is easy to see that the sign of the parameter m plays an important role in the study of the dynamics of this system. Thus, by Remark 1 we should consider the cases $m > 0$ and $m = 0$.

Case $m > 0$. In this case, the control variable $C(t)$ grows at the strictly positive constant rate $g = m/\eta$, and the question is whether the system admits an optimal balanced growth path (BGP), which is defined as follows.

Definition A1. A BGP is a path along which the (constant) growth rates of the state variables $K(t)$ and $E(t)$ are $g_K = \dot{K}(t)/K(t) > 0$ and $g_E = \dot{E}(t)/E(t) = 0$, respectively, and the ratio $C(t)/K(t)$ is constant.

According to the above definition, a BGP does not exist. Indeed, the differential equation (A.6) becomes $\dot{E}(t)/E(t) = \bar{E} - \delta\gamma - E(t) - \delta\alpha(K(t)/E(t))$, and therefore $\dot{E}(t)/E(t) = 0$ cannot be satisfied along a BGP, where $E(t)$ remains constant while $K(t)$ grows at a constant strictly positive rate.

That is, there are no optimal trajectories along which $K(t)$ and $C(t)$ grow at the same constant positive rate $g = m/\eta$ while $E(t)$ remains constant and nonzero.

We now search for the optimal trajectories along which $K(t)$ and/or $E(t)$ tend to zero in finite time.

Let $K(t)$ be increasing in an interval $I = (\underline{t}, \bar{t})$. We assume that there exists $t_1 \in I$ such that $E(t_1) = 0$. Then for $E(t) = 0, t > t_1$, the dynamics of $K(t)$ follows the differential $\dot{K}(t) = \alpha K(t) - C(t), t \geq t_1$, which has the following closed-form solution:

$$K(t) = \frac{\eta C_0}{\eta\alpha - m} e^{mt/\eta} + \frac{(\alpha\eta - m)\bar{K}_0 - \eta C_0 e^{\frac{m}{\eta}t_1}}{\alpha\eta - m} e^{\alpha(t-t_1)} \quad \forall t \geq t_1, \tag{A.7}$$

where \bar{K}_0 is the value of $K(t)$ at time $t = t_1$.

It is easy to verify that the transversality condition $\lim_{t \rightarrow \infty} \Sigma_0 e^{-\alpha t} K(t) = 0$ can be satisfied only if $\eta > m/\alpha$ and $\bar{K}_0 = \eta C_0 e^{mt_1/\eta} / (\alpha\eta - m)$ hold.

Thus, under the above conditions, the time evolution of both variables $K(t)$ and $C(t)$, which grow at a constant rate $g = m/\eta$, are trajectories optimal in the sense of Nash if and only if $E(t) = 0$ after a certain t_1 .

Figure 7 shows the only trajectory (black colour) that satisfies the above condition.

Remark A1. We note that if $K(t)$ is decreasing in I and $E(t)$ is zero, the dynamics of $K(t)$ is as in (A.7), but in this case the time evolution of $K(t)$ tends to zero in finite time. Accordingly, the transversality restriction is not necessary.

Figure 7 shows such an optimal trajectory (magenta colour), which starts in the grey region.

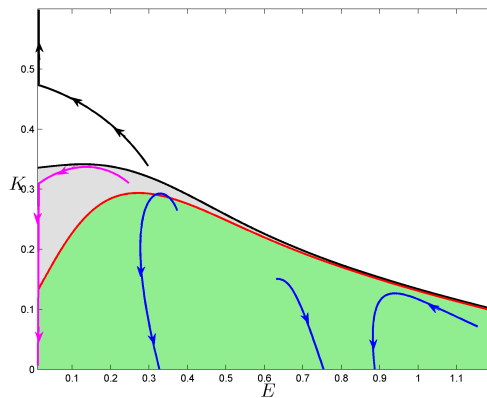


Figure 7. Numerical example of trajectories in the case of boundary arc $L(t) = 0$. Parameter values: $\alpha = 1.2, \beta = 0.15, \gamma = 0.35, \delta = 0.75, \epsilon = 0.2, \eta = 1.2, \theta = 1, \bar{E} = 1.2, C_0 = 0.4$. (Online version in colour.)

Let now t_2 be an instant of time such that $K(t_2) = 0$. Then keeping this value for all $t > t_2$, the dynamics of $E(t)$ follows $\dot{E}(t) = E(t)(\bar{E} - \delta\gamma - E(t))$ for all $t \geq t_2$, causing the state variable $E(t)$ to converge to $\bar{E} - \delta\gamma$. It is clear that there are no transversality restrictions.

Figure 7 shows some optimal trajectories (blue colour) starting from the basin of attraction defined by the green region.

Finally, Fig. 7 shows the separatrix curves (black and red colour) that divide the phase diagram in three regions.

Case $m = 0$. This case implies $C(t) = C_0 \geq \beta/\epsilon$; see (A.4). Thus, the dynamics becomes

$$\begin{aligned} \dot{K}(t) &= \alpha K(t) + \gamma E(t) - C_0, \\ \dot{E}(t) &= E(t)(\bar{E} - \delta\gamma - E(t)) - \delta\alpha K(t). \end{aligned}$$

The analysis of the above system is as in Section 4.

Appendix B: Proof of Proposition 4

We are interested in analysing the dynamics at the equilibrium point A using L_0 as bifurcation parameter. The Jacobian matrix evaluated at A is

$$J = \begin{pmatrix} \alpha & \gamma \\ -\delta\alpha & J_{22}(L_0) \end{pmatrix},$$

where $J_{22}(L_0) := -\delta\gamma + \sqrt{\bar{E}^2 - 4\delta\beta(1 - L_0)}/\epsilon$.

Its eigenvalues are the roots of the characteristic equation

$$\lambda^2 - \mathcal{T}(L_0)\lambda + \mathcal{D}(L_0),$$

where $\mathcal{T}(L_0) = \alpha + J_{12}(L_0)$ and $\mathcal{D}(L_0) = -\alpha\sqrt{\bar{E}^2 - 4\delta\beta(1 - L_0)}/\epsilon$. Thus,

$$\lambda_{1,2} = \frac{1}{2}(\mathcal{T}(L_0) \mp \sqrt{\mathcal{T}(L_0)^2 - 4\mathcal{D}(L_0)}).$$

The Hopf bifurcation condition implies

$$\mathcal{T}(L_{0H}) = 0, \quad \mathcal{D}(L_{0H}) = \omega_H^2 > 0.$$

For small $|L_{0H}|$, we can introduce

$$\mu(L_0) = \frac{1}{2}\mathcal{T}(L_0), \quad \omega(L_0) = \sqrt{\mathcal{T}(L_0)^2 - 4\mathcal{D}(L_0)},$$

and therefore obtain the following representation for the eigenvalues:

$$\lambda_1(L_0) = \mu(L_0) + i\omega(L_0), \quad \mu(L_{0H}) = 0, \quad \omega(L_{0H}) = \omega_H > 0,$$

and $\lambda_2(L_0) = \overline{\lambda_1}(L_0)$. By straightforward calculations we obtain

$$L_{0H} = 1 + \frac{\epsilon}{4\beta\delta} ((\delta\gamma - \alpha)^2 - \overline{E}^2).$$

Moreover,

$$\omega_{L_{0H}}^2 = \sqrt{\alpha(\delta\gamma - \alpha)} > 0$$

Therefore, at $L_0 = L_{0H}$ the equilibrium A has eigenvalues $\mu_{1,2}(L_{0H}) \pm i\omega(L_{0H})$ and a Hopf bifurcation occurs.

By Proposition 3, the equilibrium is stable for $L_0 < L_{0H}$ and unstable for $L_0 > L_{0H}$. We should now verify whether the genericity conditions of Theorem C1 (see Appendix C) are satisfied. The transversality condition (ii) is easy to verify:

$$\mu'(L_{0H}) = \frac{\delta\beta}{\epsilon(\delta\gamma - \alpha)} > 0.$$

To compute the first Lyapunov coefficient, we fix the parameter L_0 at its critical value L_{0H} . For this value, the equilibrium point A has coordinates

$$\begin{aligned} E_H &= \frac{1}{2}(\overline{E} - (\delta\gamma - \alpha)), & K_H &= -\frac{\gamma}{\alpha}, \\ E_H + \frac{\beta}{\alpha\epsilon}(1 - L_{0H}(1 + \epsilon)). \end{aligned}$$

We translate the origin of the coordinates to this equilibrium by the change of variables $K = K_H + x_1$ and $E = E_H + x_2$. This transforms system (22) into

$$\dot{x}_1 = \alpha x_1 + \gamma x_2, \quad \dot{x}_2 = -\delta\alpha x_1 - \alpha x_2 - x_2^2. \tag{B.1}$$

This system can be represented as [23]

$$\dot{x} = Jx + \frac{1}{2}B(x, x) + \frac{1}{6}C(x, x, x),$$

where $J = J(L_{0H})$, and the multilinear functions B and C take on the planar vectors $x = (x_1, x_2)^T$, $y = (y_1, y_2)^T$, $z = (z_1, z_2)^T$ the values

$$B(x, y) = \begin{pmatrix} 0 \\ -2x_2y_2 \end{pmatrix}$$

and $C(x, y, z) = \mathbf{0}$. We recall the matrix

$$J(L_{0H}) = \begin{pmatrix} \alpha & \gamma \\ -\delta\alpha & -\alpha \end{pmatrix}.$$

It is easy to verify that the complex vectors

$$q \sim \begin{pmatrix} 1 \\ \frac{-\alpha + i\omega}{\gamma} \end{pmatrix}, \quad p \sim \begin{pmatrix} \frac{1}{i} + \frac{i\alpha}{2\omega} \\ i\frac{\gamma}{2\omega} \end{pmatrix}$$

are proper normalised eigenvectors (i.e. $\langle p, q \rangle = 1$) of J and J^T , respectively. We now calculate

$$g_{20} = \langle p, B(q, q) \rangle = -\frac{i}{\gamma\omega}(i\omega - \alpha)^2,$$

$$g_{11} = \langle p, B(q, \bar{q}) \rangle = -\frac{i}{\gamma\omega}(\omega^2 + \alpha^2), \quad g_{21} = 0$$

and compute the first Lyapunov coefficient by

$$l_1(L_{0H}) = \frac{1}{2\omega^2} \operatorname{Re}(ig_{20}g_{11} + \omega g_{21}) = -\frac{\alpha^2\delta}{\omega^3\gamma} < 0.$$

Thus, the nondegeneracy condition (i) of Theorem C1 is satisfied as well. Therefore, a unique and stable limit cycle is obtained from the equilibrium by the Hopf bifurcation for $L_0 > L_{0H}$; see Fig. 5.

Appendix C: Hopf bifurcation theorem

Theorem C1. *We assume that a two-dimensional system*

$$\dot{\mathbf{x}} = \mathbf{f}(\mathbf{x}, \alpha), \quad \mathbf{x} \in \mathbb{R}^2, \quad \alpha \in \mathbb{R}, \tag{C.1}$$

with smooth \mathbf{f} , has for all sufficiently small $|\alpha|$ equilibrium at $\mathbf{x} = 0$ with eigenvalues

$$\lambda_{1,2} = \mu(\alpha) \pm i\omega(\alpha),$$

where $\mu(\alpha_H) = 0$ and $\omega(\alpha_H) > 0$. Moreover, the equilibrium is stable for $\alpha < \alpha_H$ and unstable for $\alpha > \alpha_0$.

Let the following conditions be satisfied:

- (i) $l_1(\alpha_H) \neq 0$, where l_1 is the first Lyapunov coefficient;
- (ii) $\mu'(\alpha_H) \neq 0$.

Then, a Hopf bifurcation occurs at the origin of the planar system (C.1) for the bifurcation value $\alpha = \alpha_H$. In particular, if $l_1 < 0$, then a unique stable limit cycle bifurcates from the origin of (C.1) as α increases from α_H ; if $l_1 > 0$, then a unique unstable limit cycle bifurcates from the origin as α decreases from α_H .

Appendix D: Poincaré compactification

The Poincaré compactification relies on the stereographic projection of a sphere onto a plane. It is used to study the behaviour of trajectories near infinity by means of the so called Poincaré sphere, introduced by Poincaré [32]. This has the advantage that singular

points at infinity are spread out along the equator of the sphere. The Poincaré compactification allows drawing the trajectories in a finite region and controls the orbits that tend to or come from infinity; see [17, 19, 24].

Let $X = P(\partial/\partial x) + Q(\partial/\partial y)$ be a polynomial vector field, where the functions P and Q are polynomials of arbitrary degree in the variables x and y , respectively.

We recall that the degree of X is d if d is the maximum of the degrees of P and Q .

The Poincaré compactification is performed as follows. First, we regard \mathbb{R}^2 as a plane in \mathbb{R}^3 defined by $(y_1, y_2, y_3) = (x, y, 1)$, and then we consider the sphere $\mathcal{S}^2 = \{y \in \mathbb{R}^3: y_1^2 + y_2^2 + y_3^2 = 1\}$, which we call here the Poincaré sphere; this sphere is tangent to \mathcal{R}^2 at the point $(0, 0, 1)$. We may divide this sphere into $H_+ = \{y \in \mathcal{S}^2: y^3 > 0\}$ (the northern hemisphere), $H_- = \{y \in \mathcal{S}^2: y^3 < 0\}$ (the southern hemisphere) and $\mathcal{S}^1 = \{y \in \mathcal{S}^2: y_3 = 0\}$ (the equator).

We consider the projection of the vector field X from \mathbb{R}^2 onto \mathcal{S}^2 given by $f^+ : \mathbb{R}^2 \rightarrow \mathcal{S}^2$ and $f^- : \mathbb{R}^2 \rightarrow \mathcal{S}^2$, where $f^+(x) = (x/\Delta, y/\Delta, 1/\Delta)$ (respectively, $f^-(x) = (-x/\Delta, -y/\Delta, -1/\Delta)$), with $\Delta = \sqrt{x^2 + y^2 + 1}$, is the intersection of the straight line passing through the point y and the north (respectively south) pole of \mathcal{S}^2 . We thus obtain an induced vector fields on each hemisphere. The induced vector field on H_+ is $\tilde{X}(y) = Df^+(x)X(x)$, where $y = f^+(x)$, and that on H_- is $\tilde{X}(y) = Df^-(x)X(x)$, where $y = f^-(x)$, with DX representing the linear part of X .

The vector field on \mathcal{S}^2 is called the *Poincaré compactification of the vector field on \mathbb{R}^2* , and it is denoted by $p(X)$.

As is usual with curved surfaces, we use charts or planes for calculation purposes. For \mathcal{S}^2 , we use the six local planes given by $U_k = \{y \in \mathcal{S}^2: y_k > 0\}$, $V_k = \{y \in \mathcal{S}^2: y_k < 0\}$ for $k = 1, 2, 3$. The corresponding local maps $\phi_k : U_k \rightarrow \mathbb{R}^2$ and $\psi_k : V_k \rightarrow \mathbb{R}^2$ are defined as $(y_m/y_k, y_n/y_k)$ for $m < n \neq k$ and $m, n \neq k$. We denote by $z = (u, w)$ the value of $\phi_k(y)$ or $\psi_k(y)$ for any k , such that (u, v) will take on different values depending on the plane under consideration. For points of \mathcal{S}^1 in a chart, we have $v = 0$.

The expression for $p(X)$ in the local chart U_1 is given by

$$\dot{u} = v^d \left[-uP\left(\frac{1}{v}, \frac{u}{v}\right) + Q\left(\frac{1}{v}, \frac{u}{v}\right) \right], \quad \dot{v} = -w^{d+1}P\left(\frac{1}{v}, \frac{u}{v}\right).$$

On the chart U_2 , the expression is

$$\dot{u} = v^d \left[P\left(\frac{1}{v}, \frac{u}{v}\right) - uQ\left(\frac{1}{v}, \frac{u}{v}\right) \right], \quad \dot{v} = -w^{d+1}Q\left(\frac{1}{v}, \frac{u}{v}\right),$$

and on U_3 , it is

$$\dot{u} = P(u, v), \quad \dot{v} = Q(u, v).$$

For the other three planes V_i , $i = 1, 2, 3$, the expression is the same as for U_i multiplied by $(-1)^{d-1}$ for $i = 1, 2, 3$.

Appendix E: Nilpotent theorem

Theorem E1. Let $(0, 0)$ be an isolated singular point of the vector field X given by

$$\dot{u} = v + X(u, v), \quad \dot{v} = Y(u, v),$$

where X and Y are analytic in a neighbourhood of the point $(0, 0)$ and $X(0, 0) = Y(0, 0) = 0$. Let $v = F(u)$ be the solution of the equation $v + X(u, v) = 0$ in a neighbourhood of $(0, 0)$. Moreover, we define

$$f(u) := Y(u, F(u)) = a_1 u^\alpha + O(u^\alpha), \quad a_1 \neq 0, \alpha \geq 2;$$

$$\phi(u) := \left(\frac{\partial X}{\partial u} + \frac{\partial Y}{\partial v} \right) (u, F(u)) = b_1 u^\beta + O(u^\beta), \quad b_1 \neq 0, \beta \geq 1.$$

Then the following hold:

- (a) If α is even, then
 - (a1) if $\alpha > 2\beta + 1$, then $(0, 0)$ is a saddle-node;
 - (a2) if either $\alpha < 2\beta + 1$ or $\phi = 0$, then $(0, 0)$ is a critical point whose neighbourhood is the union two hyperbolic sectors;
- (b) if α is odd and $a > 0$, then $(0, 0)$ is a saddle;
- (c) if α is odd and $a < 0$, then
 - (c1) if either $\alpha > 2\beta + 1$ and β is even, or $\alpha = 2\beta + 1$, β is even and $b^2 + 4a \times (\beta + 1) \geq 0$, then $(0, 0)$ is a node;
 - (c2) if either $\alpha > 2\beta + 1$ and β is odd, or $\alpha = 2\beta + 1$, β is odd and $4a(\beta + 1) \geq 0$, then $(0, 0)$ is the union of one hyperbolic sector and one elliptic sector;
 - (c3) if either $\alpha = 2\beta + 1$ and $b^2 + 4a(\beta + 1) \leq 0$, or $\alpha < 2\beta + 1$ or $\phi = 0$, then $(0, 0)$ is a focus or a centre.

References

1. A.F. Andreev, Investigation of the behavior of the integral curves of a system of two differential equations in the neighbourhood of a singular point, in *Twelve Papers on Function Theory, Probability and Differential Equations*, Transl., Ser. 2, Am. Math. Soc., Vol. 8, AMS, Providence, RI, 1958, pp. 183–207.
2. A. Antoci, M. Galeotti, P. Russu, Poverty trap and global indeterminacy in a growth model with open access natural resources growth model, *J. Econ. Theory*, **146**(2):569–591, 2011.
3. A. Antoci, M. Galeotti, P. Russu, Global analysis and indeterminacy in a two-sector growth model with human capital, *Int. J. Econ. Theory*, **10**(4):313–338, 2014.
4. A. Antoci, M. Sodini, L. Zarri, Relational consumption and nonlinear dynamics in an overlapping generations model, *Decis. Econ. Finance*, **37**(1):137–158, 2014.
5. A.D. Ayong Le Kama, Sustainable growth, renewable resources and pollution, *J. Econ. Dyn. Control*, **25**(12):1911–1918, 2001.

6. J. Benhabib, K. Nishimura, T. Shigoka, Bifurcation and sunspots in the continuous time equilibrium model with capacity utilization, *Int. J. Econ. Theory*, **4**(2):337–355, 2008.
7. R.L. Bennet, R.E. Farmer, Indeterminacy with non-separable utility, *J. Econ. Theory*, **93**(1):118–143, 2000.
8. P. Berck, J.M. Perloff, An open-access fishery with rational expectations, *Econometrica*, **52**(2):489–506, 1984.
9. G.I. Bischi, F. Lamantia, Harvesting dynamics and unprotected areas, *J. Econ. Behav. Organ.*, **62**(3):348–370, 2007.
10. R. Boucekkine, A. Pommerety, F. Prieurz, On the timing and optimality of capital controls: Public expenditures, debt dynamics and welfare, *Int. J. Econ. Theory*, **9**(1):101–112, 2013.
11. G.M. Brown, Renewable natural resource management and use without markets, *J. Econ Lit.*, **38**(4):875–914, 2000.
12. O.A. Carboni, P. Russu, Linear production function, externalities and indeterminacy in a capital-resource growth model, *J. Math. Econ.*, **49**(5):422–428, 2013.
13. O.A. Carboni, P. Russu, A model of economic growth with public finance: Dynamics and analytic solution, *Journal of Economics and Financial Issues*, **3**(1):1–13, 2013.
14. O.A. Carboni, P. Russu, Global indeterminacy in a tourism sector model, *Nonlinear Stud.*, **21**(3):375–385, 2014.
15. S. D'Alessandro, Non-linear dynamics of population and natural resources: the emergence of different patterns of development, *Ecol. Econ.*, **62**(3–4):473–481, 2007.
16. R. Damania, J. Hatch, Protecting eden: Markets or government?, *Ecol. Econ.*, **53**(3):339–351, 2015.
17. F. Dumortier, J.C. J. Llibre, J.C. Artès, *Qualitative Theory of Planar Differential Systems*, Springer, Berlin, Heidelberg, 2006.
18. L. Eliasson, S. Turnovsky, Renewable resources in an endogenously growing economy: Balanced growth and transitional dynamics, *J. Environ. Econ. Manage.*, **48**(3):1018–1049, 2004.
19. E. González-Olivares, H. Meneses-Alcay, B. González-Yanez, J. Mena-Lorca, A. Rojas-Palma, R. Ramos-Jiliberto, Multiple stability and uniqueness of the limit cycle in a Gause-type predator-prey model considering the Allee effect on prey, *Nonlinear Anal., Real World Appl.*, **12**(6):2931–2942, 2011.
20. L. Gori, M. Sodini, Nonlinear dynamics in an OLG growth model with young and old agents labour supply: The role of public health expenditure, *J. Comp. Econ.*, **38**(3):261–275, 2011.
21. J.I. Itaya, Can environmental taxation stimulate growth? the role of indeterminacy in endogenous growth models with environmental externalities, *J. Econ. Dyn. Control*, **32**(4):1156–1180, 2008.
22. P. Krugman, History versus expectations, *Q. J. Econ.*, **106**(2):651–667, 1991.
23. Y. Kuznetsov, *Elements of Applied Bifurcation Theory*, Springer-Verlag, New York, 1998.
24. Y. Liu, Dynamics at infinity and the existence of singularly degenerate heteroclinic cycles in the conjugate Lorenz-type system, *Nonlinear Anal., Real World Appl.*, **13**(6):2466–2475, 2012.

25. R.E. López, Structural change, poverty and natural resource degradation, in G. Atkinson, S. Dietz, E. Neumayer (Eds.), *Handbook of Sustainable Development*, pp. 220–239, Edward Elgar Publishing, Cheltenham, UK, Northampton, MA, 2007.
26. R.E. López, G. Anríquez, S. Gulati, Structural change and sustainable development, *J. Environ. Econ. Manage.*, **53**(3):307–322, 2007.
27. M. Makris, Necessary conditions for infinite-horizon discounted two-stage optimal control problems, *J. Econ. Dyn. Control*, **25**(12):1935–1950, 2011.
28. K. Matsuyama, Increasing returns, industrialization, and indeterminacy of equilibrium, *Q. J. Econ.*, **106**(2):617–650, 1991.
29. P. Mattana, K. Nishimura, T. Shigoka, Homoclinic bifurcation and global indeterminacy of equilibrium in a two-sector endogenous growth model, *Int. J. Econ. Theory*, **5**(1):25–47, 2009.
30. S.F. McWhinnie, The tragedy of commons in international fisheries: an empirical examination, *J. Environ. Econ. Manage.*, **57**(3):321–333, 2009.
31. K. Mino, Indeterminacy and endogenous growth with social constant returns, *J. Econ. Theory*, **97**(1):203–222, 2001.
32. H. Poincaré, Sur l'intégration des équations différentielles du premier ordre et du premier degré, *Rend. Circ. Mat. Palermo*, **5**(1):161–191, 1891.
33. F. Wirl, Stability and limit cycles in one-dimensional dynamic optimizations of competitive agents with a market externality, *J. Evol. Econ.*, **7**(1):73–89, 1997.